

Trapping Light with Grating Defects

R. H. Goodman, R. E. Slusher, M. I. Weinstein, and M. Klaus

ABSTRACT. Gap solitons are localized traveling waves that exist in Bragg grating optical fibers. We demonstrate a family of grating defects that support linear and nonlinear standing wave modes, and show numerically that these defect modes may be used to trap the energy from a gap soliton. A mechanism involving a nonlinear resonance is proposed to explain why trapping occurs in some situations and not in others.

Solitons, traveling waves which propagate without distortion, have long been considered candidates for the carriers of information in long distance optical fibers. Bragg grating fibers are specialized optical fibers in which the index of refraction is a periodic function in the direction of light propagation. They support a family of traveling waves known as gap solitons first described in [1, 3]. These have many properties that make them attractive as carriers of information in optical data processing units, such as multiplexer/demultiplexers or buffers. For a survey of gap solitons in Bragg gratings, see [4].

1. Nonlinear Coupled Mode Equations and Gap Solitons

The evolution of the electric field in the fiber may be modeled by a one-dimensional Maxwell's equation

$$(1) \quad \partial_t^2 [n^2(z)E(z, t)] = \partial_z^2 E,$$

nondimensionalized to make the speed of light $c = 1$ and the refractive index n is:

$$(2) \quad n = 1 + \epsilon \left(\frac{1}{2}W(\epsilon z) + \nu(\epsilon z) \cos(2k_B z + 2\Phi(\epsilon z)) + |E|^2 \right).$$

If $W \equiv \Phi \equiv 0$ and $\nu \equiv 1$, then the grating is uniform—these terms represent, respectively, local variations in the index of refraction, the grating phase, and the grating strength. The Bragg wavenumber k_B is chosen to match the wavenumber of laser light propagating through the fiber.

We now make a *multiple scales ansatz* [8, 9], choosing the carrier wavenumber in *Bragg resonance* with the medium:

$$(3) \quad E = \sqrt{\epsilon} \left(E_+(\epsilon z, \epsilon t) e^{i(k_B(z-t) + \Phi)} + E_-(\epsilon z, \epsilon t) e^{-i(k_B(z+t) + \Phi)} \right) + O(\epsilon^{3/2}).$$

1991 *Mathematics Subject Classification*. Primary 78A60, 35Q60.

Key words and phrases. Optics, traveling waves.

Research completed under NSF University–Industry cooperative fellowship DMS-99-01897 at Lucent Technologies Bell Laboratories and Princeton University.

Then the method of multiple scales yields equations for the evolution of the wave envelopes E_+ and E_- in terms of the slow variables $Z = \epsilon z$ and $T = \epsilon t$:

$$(4) \quad \begin{aligned} i\partial_T E_+ + i\partial_Z E_+ + \kappa(Z)E_- + V(Z)E_+ + \Gamma(|E_+|^2 + 2|E_-|^2)E_+ &= 0 \\ i\partial_T E_- - i\partial_Z E_- + \kappa(Z)E_+ + V(Z)E_- + \Gamma(|E_-|^2 + 2|E_+|^2)E_- &= 0, \end{aligned}$$

The functions $\kappa(Z)$ and $V(Z)$ are defined in terms of the modulations W , ν and Φ , and the nonlinearity strength Γ may be set equal to one by a rescaling of E_{\pm} [7]. The κ term arises due to the existence of the grating and couples the forward and backward traveling components of the electric field to each other.

In the absence of modulations $\kappa(Z) \equiv \bar{\kappa}$, a constant, and $V(Z) \equiv 0$. This system is known as the nonlinear coupled mode equations (NLCME). The linearized constant coefficient equations have solutions of the form

$$\begin{pmatrix} E_+(Z, T) \\ E_-(Z, T) \end{pmatrix} = \begin{pmatrix} e_+ \\ e_- \end{pmatrix} e^{i(kZ - \omega T)}$$

where k and ω satisfy the linear dispersion relation $\omega = \pm\sqrt{\bar{\kappa}^2 + k^2}$, implying a band gap in the spectrum of the linearized equation with no frequency $\omega \in (-\bar{\kappa}, \bar{\kappa})$.

The (constant coefficient) NLCME support a family of traveling pulses called gap solitons [1, 3], parameterized by a velocity v and a detuning parameter δ ($|v| < 1$ and $0 \leq \delta \leq \pi$):

$$(5) \quad E_{\pm} = \pm\Delta^{\mp 1} \alpha \sqrt{\frac{\bar{\kappa}}{2}} \sin \delta e^{i(\eta + \sigma)} \operatorname{sech}(\theta \mp i\delta/2) ;$$

where:

$$\begin{aligned} \Delta &= \left(\frac{1-v}{1+v}\right)^{\frac{1}{4}} ; \quad \alpha = \sqrt{\frac{2(1-v^2)}{3-v^2}} ; \quad e^{i\eta} = \left(-\frac{e^{2\theta} + e^{-i\delta}}{e^{2\theta} + e^{i\delta}}\right)^{\frac{2v}{3-v^2}} ; \\ \theta &= \frac{\bar{\kappa}}{\sqrt{1-v^2}}(\sin \delta)(z - vt) ; \quad \sigma = \frac{\bar{\kappa}}{\sqrt{1-v^2}}(\cos \delta)(vz - t). \end{aligned}$$

The equations show gap solitons may move at any velocity v below the speed of light, although this has been difficult to achieve in the lab. Experiments in fibers have produced pulses as slow as half the speed of light, and theorists estimate that this could be reduced to $c/10$ [2, 6]. Of special interest are stationary ($v = 0$) pulses which could be used as bits in an optical memory system.

We define the total intensity of a pulse by its squared L^2 norm,

$$(6) \quad I_{\text{tot}} = \int_{-\infty}^{\infty} (|E_+|^2 + |E_-|^2) dZ = \frac{4(1-v^2)\delta}{(3-v^2)}.$$

Gap solitons with $v = 0$ form a family of nonlinear standing waves. From (5), these have internal frequency $\omega = \bar{\kappa} \cos \delta$. Figure 1 shows I_{tot} as a function of frequency for stationary solitons. As δ varies from zero to π , the frequency varies from the right to the left edge of the band gap.

2. Linear and Nonlinear Defect Modes

The variable coefficient terms $\kappa(Z)$ and $V(Z)$ in (4) may serve as a potential. We may construct potentials that support defect modes, localized solutions to the

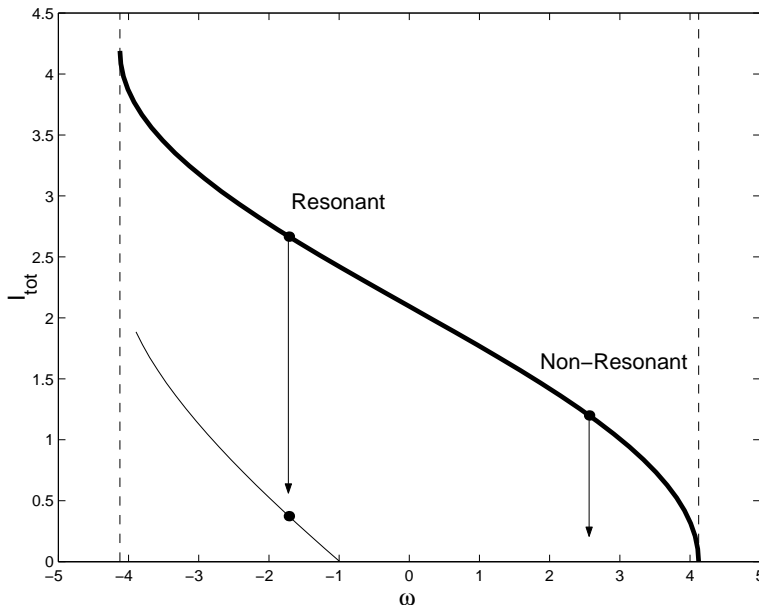


FIGURE 1. Intensity as a function of frequency for the stationary gap soliton (thick line) and for the nonlinear defect mode of the defect with parameters $\omega = -1$, $k = 4$, $n = 1$ (thin line).

linearized form of (4) (obtained by setting $\Gamma = 0$) of the form

$$(7) \quad \begin{pmatrix} E_+(Z, T) \\ E_-(Z, T) \end{pmatrix} = \begin{pmatrix} E_+(Z) \\ E_-(Z) \end{pmatrix} e^{-i\omega T}.$$

In [7], we construct a three parameter family of defects of the form

$$\kappa(Z) = \sqrt{\omega^2 + n^2 k^2 \tanh^2(kZ)}; \quad V(Z) = \frac{\omega n k^2 \operatorname{sech}^2(kZ)}{2(\omega^2 + n^2 k^2 \tanh^2(kZ))}.$$

for which standing wave solutions exist of the form:

$$(8) \quad E_{\pm} = e^{\pm \frac{i}{2} \arctan \frac{nk \tanh(kZ)}{\omega}} \operatorname{sech}^n(kZ) e^{-i\omega t}.$$

It was found numerically that for $n > 1$, the defect supports additional eigenmodes with eigenvalues given by

$$(9) \quad \omega_{\pm r} = \pm \sqrt{\omega^2 + (2nr - r^2)k^2}; \quad 1 \leq r < n.$$

In appendix A, the eigenvalues, and their associated eigenfunctions are derived.

In the nonlinear eigenvalue problem, the linear solution applies in the limit as $I_{tot} \rightarrow 0$. As the intensity is increased, the frequency moves toward the left edge of the band gap, as is seen in the numerical calculation pictured in figure 1.

3. Numerical Experiments in Gap Soliton Capture

Away from the defect at $Z = 0$, the variable coefficients satisfy $\kappa(Z) \rightarrow \bar{\kappa}$ and $V(Z) \rightarrow 0$. Therefore, away from the defects, gap solitons may propagate. Given the difficulty of creating low speed or stationary pulses, we performed a series of

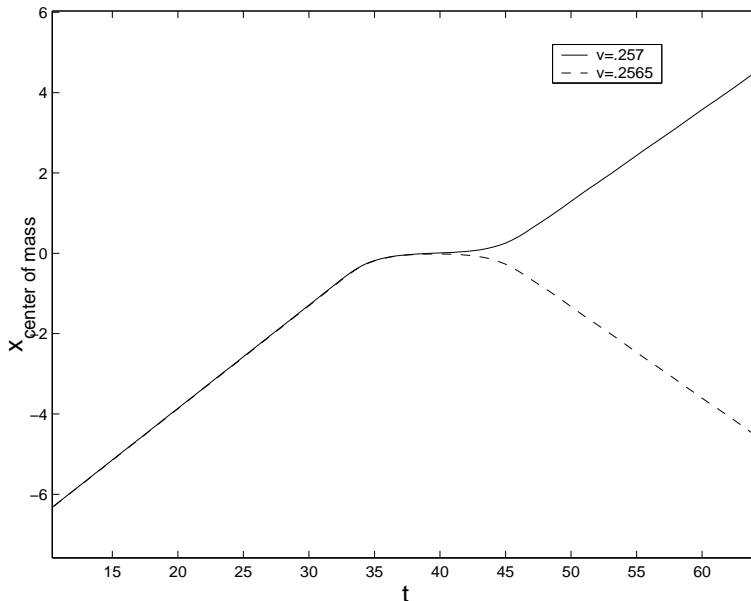


FIGURE 2. The positions of solitons which are transmitted (solid) and reflected (dashed) at speeds close to the critical speed.

numerical experiments in which gap solitons were initialized far from, and propagating toward, the defect, attempting to capture gap solitons using the defects. An interesting and unexpected phenomenon was seen in these experiments, depending on the parameters used to define the defects and pulses. In certain parameter regimes, the soliton was either coherently reflected or transmitted, depending on the velocity v of the incoming soliton; see figure 2. In these cases, the pulse remains remarkably intact following the interaction, so only its position has been shown. In other parameter regimes, much of the soliton’s energy is captured at the defect at slow velocities, while at larger velocities the soliton largely passes the defect, albeit with reduced speed; see figure 3. As the soliton’s speed is increased, the fraction of captured energy is decreased. A larger set of numerical experiments as well as estimates of the physical dimensions of the pulses and defects is presented in [7].

The hypothesized explanation for the difference between the two cases outlined above is shown figure 1. The two cases are pictured schematically along with the labels “Nonresonant” and “Resonant”. In both cases the defect is defined by the parameters $(\omega, k, n) = (-1, 4, 1)$. The difference lies in the parameter δ which is 1 in the first (reflection/transmission) case labeled “Nonresonant” and 2 in the second (capture/transmission) case labeled “Resonant.” In all cases, the velocity of the incoming soliton is initialized to $v \ll 1$, so its internal frequency is approximately $\omega = \bar{\kappa} \cos \delta$ and its total intensity is approximately $I_{tot} = 4\delta/3$. For $\delta = 0$, this is represented by a point in the lower-right corner of the upper curve, moving up and to the left along the curve as δ is increased. We compare the point on the gap soliton curve with the defect mode curve below it. Trapping is then well predicted by the following principle.

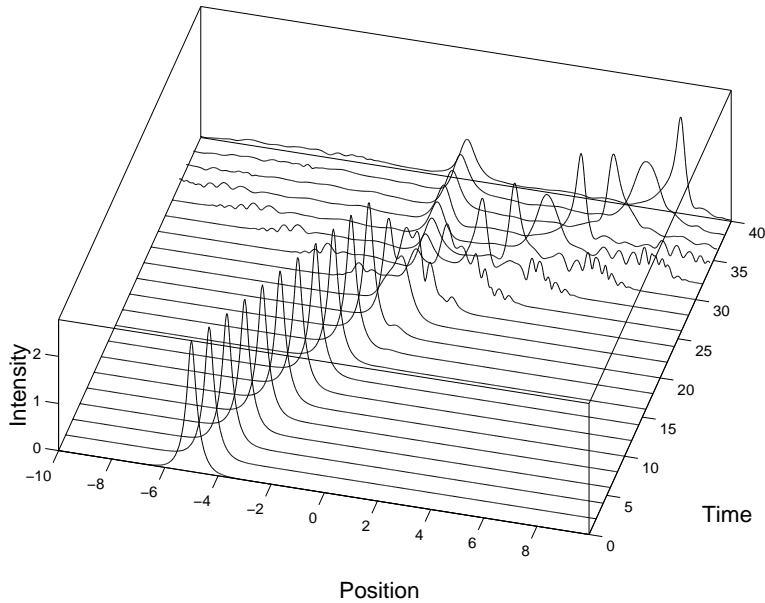


FIGURE 3. A soliton with higher intensity has some energy captured at the same speed at which the soliton is reflected in the previous example

Principle governing soliton-defect interactions: *Consider a gap soliton incident on a defect with sufficiently low incident velocity. The gap soliton will transfer its energy to a nonlinear defect mode, and thereby be trapped, if there exists a nonlinear defect mode of the same frequency (resonance) **and** lower total intensity (energetic accessibility). Otherwise, the gap soliton energy will be reflected and/or transmitted.*

It should be stressed that this principle is approximate and that figure 1 is a schematic. The defect mode that is captured may oscillate with frequency higher or lower than that of the incoming soliton.

As evidence for this principle, the numerically computed solution is projected onto the linear defect mode. The amplitude of this projection is plotted in figure 4 for both the reflected (nonresonant) and a captured (resonant) incoming soliton. In the upper picture both the L^2 norm of the computed solution and of its projection onto the linear defect mode are computed. The defect mode is weakly and briefly excited, but quickly returns its energy to the soliton. In the lower curve, the same quantities are plotted for the case of capture. The L^2 -norm, which is conserved by the PDE dynamics, is reduced via loss of energy at the endpoints of the computation. By the end of the run, however, almost all of the solution can be accounted for by its projection onto the linear defect mode. This demonstrates that capture takes place via a resonant transfer of energy to the nonlinear defect mode, rather than via a slowing of the soliton.

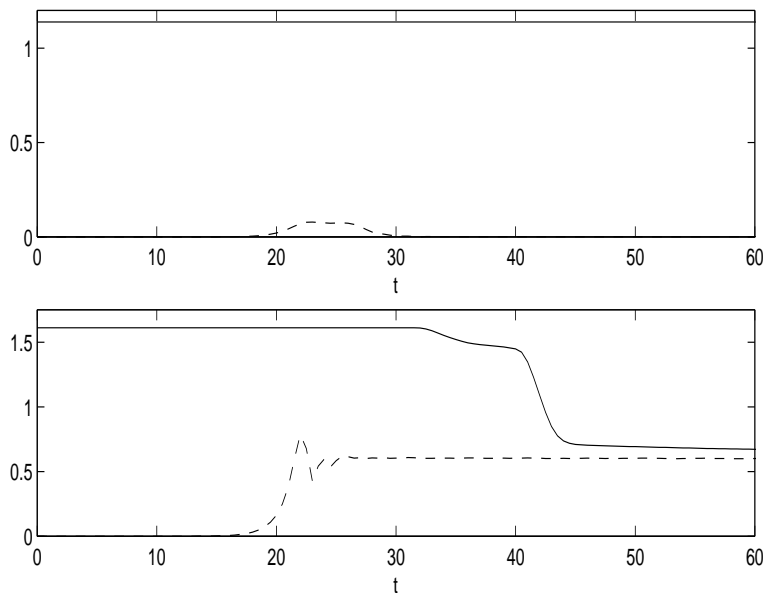


FIGURE 4. The L^2 norms of the computed solutions (solid) and of their projections onto the linear defect modes (dashed) for the nonresonant reflected soliton (top) and resonant captured soliton (bottom).

4. Further Experiments and Conclusion

Two difficulties remain with the above results. First, figure 1 shows that only solitons with a large δ parameter—and thus fairly intense light—can be captured by the defect used in that experiment. This may be addressed by altering the defect in two ways. First, by simply changing the defect parameter from $\omega = -1$ to $\omega = 1$, the defect mode bifurcation curve moves significantly to the right, solitons with lower intensities (further to the right on the upper curve) to be captured, as shown in the left image of figure 5. Solitons of even smaller intensity can be captured by using the multi-mode defect modes with $n > 1$ described in section 2. The defect defined by the parameters $(\omega, k, n) = (-1, 2, 2)$, which has the same value of $\bar{\kappa}$ and thus the same spectral gap, but possesses 3 defect modes. This defect can capture energy from solitons of even lower intensity, as shown in the right image of figure 5. Of course when multiple modes are able to interact, the set of possible behaviors becomes much richer. A second difficulty is that energy continues to radiate from the defect after it is captured. This is a more fundamental issue.

Gap solitons in Bragg gratings are a fertile subject in nonlinear fiber optics and all-optical communications system. We have investigated how such nonlinear traveling waves may be made to transfer their energy to localized modes at specified defect locations. We have performed numerical experiments and formulated a principle whereby solitons are trapped by transferring their energy to a defect mode when they are resonant with an appropriate nonlinear defect mode.

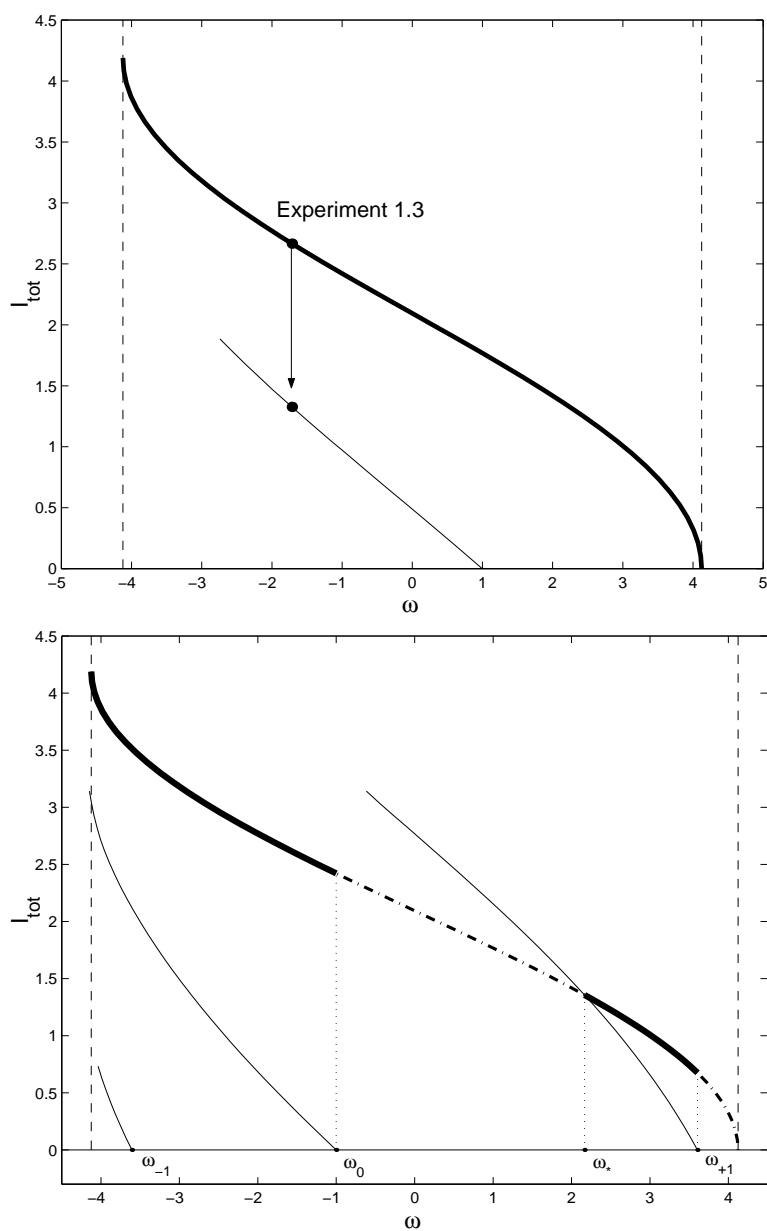


FIGURE 5. Bifurcation curves for the defects with parameters $(\omega, k, n) = (1, 4, 1)$ (left) and $(-1, 2, 2)$ (right). In the right graph, solitons on the darkened portions of the gap soliton curve may be trapped by the nonlinear defect modes beneath them.

Appendix A. Calculation of additional eigenvalues and eigenfunctions

We seek solutions of the form (7) to the linearized ($\Gamma = 0$) form of NLCME (4). Letting $\vec{F} = \begin{pmatrix} E_+(z) \\ E_-(z) \end{pmatrix}$ and

$$u(z) = -i\kappa(z) \exp\left(-2i \int_0^z V(\zeta) d\zeta\right) = -kn \tanh kz - i\omega \quad n \geq 1; k, \omega \in \mathbb{R}$$

rewrite (4) as a Zakharov-Shabat eigenvalue problem:

$$(10) \quad \partial_z \vec{F} = \begin{pmatrix} i\Omega & u(z) \\ \bar{u}(z) & -i\Omega \end{pmatrix} \vec{F}.$$

In [7], one eigenvector, with eigenvalue $\Omega = \omega$ is constructed. If $n > 1$, additional eigenvalues given in (9) discovered found numerically. Here we find these eigenvalues and their corresponding eigenvectors explicitly.

First, rewrite (10) as

$$(11) \quad H\vec{F} \equiv \begin{pmatrix} -i\partial_z & iu \\ -i\bar{u} & i\partial_z \end{pmatrix} \vec{F} = \Omega\vec{F}.$$

The operator H is self-adjoint, and thus has real spectrum. Then

$$(12) \quad H^2 F = \Omega^2 F$$

where

$$(13) \quad H^2 = \begin{pmatrix} -\partial_z^2 + |u|^2 & u_z \\ \bar{u}_z & -\partial_z^2 + |u|^2 \end{pmatrix} = \begin{pmatrix} -\partial_z^2 + |u|^2 & u_z \\ u_z & -\partial_z^2 + |u|^2 \end{pmatrix}$$

since $u_z = -k^2 n \operatorname{sech}^2 kz$ is real.

Diagonalize equation (12) by letting $\vec{G} = U\vec{F} \equiv \begin{pmatrix} 1 & 1 \\ 1 & -1 \end{pmatrix} \vec{F}$. Then

$$(14) \quad A\vec{G} \equiv \begin{pmatrix} A_+ & 0 \\ 0 & A_- \end{pmatrix} \equiv \begin{pmatrix} -\partial_z^2 + |u|^2 + u_z & 0 \\ 0 & -\partial_z^2 + |u|^2 - u_z \end{pmatrix} \vec{G} = \Omega^2 \vec{G},$$

where $A = UH^2U^{-1}$. The spectrum is simply the union of the spectra of the two diagonal terms, i. e. of $-\partial_z^2 + |u|^2 \pm u_z$. Thus we may study separately the two equations:

$$(15a) \quad -\partial_z^2 G_1 - k^2 n(n+1) \operatorname{sech}^2(kz) G_1 = (\Omega^2 - \omega^2 - k^2 n^2) G_1;$$

$$(15b) \quad -\partial_z^2 G_2 - k^2 n(n-1) \operatorname{sech}^2(kz) G_2 = (\Omega^2 - \omega^2 - k^2 n^2) G_2.$$

The spectrum of the Schrödinger equation with a sech^2 potential is well known [5]. For equation (15a),

$$\Omega^2 - \omega^2 - k^2 n^2 = -k^2(n+1-p)^2, \quad p = 1, \dots, n$$

and for (15b),

$$\Omega^2 - \omega^2 - k^2 n^2 = -k^2(n-r)^2, \quad r = 1, \dots, n-1.$$

When $p = 1$, only the first equation has a solution, corresponding to $\Omega^2 = \omega^2$. For $r = p-1$, the eigenvalues of (15a) and (15b), coincide, yielding a pair of eigenvalues

$$\Omega = \pm \sqrt{\omega^2 + k^2 n^2 - k^2(n-r)^2} = \pm \sqrt{\omega^2 + k^2(2nr - r^2)}$$

of (10) in agreement with the numerical observation (9).

In order to determine the correct signs for the eigenvalues of H , we need to look closely at the eigenfunctions of (15). For equation (15a), the solution is

$$G_{1,p} = \begin{cases} \cosh^{n+1}(kz)F(a, b, \frac{1}{2}, -\sinh^2 kz) & p \text{ odd,} \\ \cosh^{n+1}(kz) \sinh(kz)F(a + \frac{1}{2}, b + \frac{1}{2}, \frac{3}{2}, -\sinh^2 kz) & p \text{ even} \end{cases}$$

where $a = \frac{p}{2}$, $b = n + 1 - \frac{p}{2}$, and $F(a, b, c, z)$ is the hypergeometric function. For equation (15b), the solution is

$$G_{2,r} = \begin{cases} \cosh^n(kz)F(\tilde{a}, \tilde{b}, \frac{1}{2}, -\sinh^2 kz) & r \text{ odd,} \\ \cosh^n(kz) \sinh(kz)F(\tilde{a} + \frac{1}{2}, \tilde{b} + \frac{1}{2}, \frac{3}{2}, -\sinh^2 kz) & r \text{ even} \end{cases}$$

where $\tilde{a} = \frac{r}{2}$, and $\tilde{b} = n - \frac{r}{2}$. If n is an integer, this can be simplified using Legendre functions [5].

Note that from (10), it follows that:

$$\begin{aligned} F_1'(0) &= i\Omega F_1(0) - i\omega F_2(0); \\ F_2'(0) &= i\omega F_1(0) - i\Omega F_2(0), \end{aligned}$$

so that

$$(16) \quad \begin{aligned} G_1'(0) &= i(\Omega + \omega)G_2(0); \\ G_2'(0) &= i(\Omega - \omega)G_1(0). \end{aligned}$$

Now let's look at the various eigenvalues: First consider the eigenvalue of equation (15a) with $p = 1$ so that $\Omega^2 = \omega^2$, then

$$\begin{aligned} G_1 &= \cosh^{n+1}(kz)F(\frac{1}{2}, n + \frac{1}{2}, \frac{1}{2}, -\sinh^2 kz) \\ &= \cosh^{n+1}(kz)(1 + \sinh^2 kz)^{-n-\frac{1}{2}} \\ &= \operatorname{sech}^n kz, \end{aligned}$$

as $F(\frac{1}{2}, n + \frac{1}{2}, \frac{1}{2}, z) = (1 - z)^{-n-\frac{1}{2}}$. Then, as $G_2 = 0$ for this case, we have

$$F_1 = F_2 = \frac{1}{2}G_1 = \frac{1}{2}\operatorname{sech}^n kz.$$

Note that G_1 is even with $G_1(0) = 1$. Thus, by the second equation of (16), $(\Omega - \omega) = 0$, or $\Omega = \omega$.

Now if $p > 1$ and p is even, and let $r = p - 1$, then,

$$\begin{aligned} G_1 &= \cosh^{n+1}(kz) \sinh(kz)F(a + \frac{1}{2}, b + \frac{1}{2}, \frac{3}{2}, -\sinh^2 kz) \\ G_2 &= \cosh^n(kz)F(\tilde{a}, \tilde{b}, \frac{1}{2}, -\sinh^2 kz) \end{aligned}$$

and vectors of the form $\begin{pmatrix} \alpha G_1 \\ \beta G_2 \end{pmatrix}$ span the eigenspace corresponding to the eigenvalue

$$\Omega^2 = \omega^2 + k^2 n^2 - k^2(n + 1 - p)^2 = \omega^2 + k^2 n^2 - k^2(n - r)^2$$

of A . Let $\Omega_{\pm} = \pm|\Omega|$. Then either of Ω_{\pm} may be an eigenvalue of (11). Since G_1 is odd and G_2 is even, the first equation of (16) yields:

$$\alpha G_1'(0) = \alpha k = i(\Omega_{\pm} + \omega)G_2(0) = i(\Omega_{\pm} + \omega)\beta.$$

Setting $\beta = k$ and $\alpha_{\pm} = i(\Omega_{\pm} + \omega)$ yields the eigenfunction

$$\vec{F}_{\pm} = \begin{pmatrix} \alpha_{\pm} G_1 \\ \beta G_2 \end{pmatrix}$$

corresponding to eigenvalue Ω_{\pm} . A similar computation may be performed for $p > 1$ odd.

References

1. A. B. Aceves and S. Wabnitz, *Self induced transparency solitons in nonlinear refractive periodic media*, Phys. Lett. A **141** (1989), 37–42.
2. N. G. R. Broderick, D. J. Richardson, and M. Ibsen, *Nonlinear switching in a 20-cm-long fiber Bragg grating*, Opt. Lett. **25** (2000), 536–538.
3. D. N. Christodoulides and R. I. Joseph, *Slow Bragg solitons in nonlinear periodic structures*, Phys. Rev. Lett. **62** (1989), 1746–1749.
4. C. M. de Sterke and J. E. Sipe, *Gap solitons*, Progress in Optics **33** (1994), 203–260.
5. P. G. Drazin and R. S. Johnson, *Solitons: An introduction*, Cambridge University Press, 1993.
6. B. J. Eggleton, C. M. de Sterke, and R. E. Slusher, *Nonlinear pulse propagation in Bragg gratings*, J. Opt. Soc. Am. B. **14** (1997), no. 11, 2980–2992.
7. R. H. Goodman, R. E. Slusher, and M. I. Weinstein, *Stopping light on a defect*, J. Opt. Soc. Amer. B **19** (2001), 1635–1652.
8. R. H. Goodman, M. I. Weinstein, and P. J. Holmes, *Nonlinear propagation of light in one dimensional periodic structures*, J. of Nonlinear Sci. **11** (2001), 123–168.
9. J. Kevorkian and J. Cole, *Multiple Scale and Singular Perturbation Methods*, Springer-Verlag, New York, 1996.

DEPARTMENT OF MATHEMATICAL SCIENCES, NEW JERSEY INSTITUTE OF TECHNOLOGY, NEWARK, NJ 07102

E-mail address: `goodman@njit.edu`

OPTICAL PHYSICS RESEARCH, BELL LABORATORIES–LUCENT TECHNOLOGIES, MURRAY HILL, NJ 07974

E-mail address: `res@lucent.com`

DEPARTMENT OF APPLIED PHYSICS AND APPLIED MATHEMATICS, COLUMBIA UNIVERSITY, NEW YORK, NY 10027 AND MATHEMATICAL SCIENCES RESEARCH, BELL LABORATORIES–LUCENT TECHNOLOGIES, MURRAY HILL, NJ 07974

E-mail address: `miw2103@columbia.edu`

DEPARTMENT OF MATHEMATICS, VIRGINIA POLYTECHNIC INSTITUTE AND STATE UNIVERSITY, BLACKSBURG, VA 24061

E-mail address: `klaus@math.vt.edu`